ELECTROPORATION OF CELL MEMBRANE VISUALIZED UNDER A PULSED-LASER FLUORESCENCE MICROSCOPE

KAZUHIKO KINOSITA, JR.,* IKUO ASHIKAWA,* NOBUYUKI SAITA,* HIDEYUKI YOSHIMURA,‡ HIROYASU ITOH,§ KUNIAKI NAGAYAMA,‡ AND AKIRA IKEGAMI*

**The Institute of Physical and Chemical Research, Hirosawa, Wako-shi, Saitama 351-01, Japan; ‡Biometrology Lab, JEOL Ltd., Nakagami, Akishima-shi, Tokyo 196, Japan; and §Tsukuba Research Laboratory, Hamamatsu Photonics K. K., Tokodai, Tsukuba-shi, Ibaraki 300-26, Japan*

ABSTRACT Controlled permeability can be conferred to cell membranes by exposing cells to a microsecond electric pulse of sufficient intensity (electroporation). By constructing a fluorescence microimaging system with a submicrosecond time resolution we have been able to resolve temporally and spatially the events in a single cell under a microsecond electric pulse. An enormous membrane conductance, corresponding to a loss of 0.01–0.1% of the membrane area, was observed in those membrane regions where the transmembrane potential induced by the electric pulse exceeded a critical value. The conductance decreased to a low level in a submillisecond after the pulse, leaving a moderately electroporated cell.

INTRODUCTION

A recent development in cell technology is the application of high-voltage pulses to living cells (1, 2). The pulse treatment renders the cell permeable apparently by the formation of aqueous pores in the cell membrane (electroporation or electropermeabilization). The high permeability allows the manipulation of cellular contents. If two or more cells are in contact with each other, the pulse-induced change in membrane structure eventually leads to the fusion of the cells (electrofusion). Giant cells or hybrid cells can be produced. The electroporation and electrofusion are becoming useful tools in experiments and application. The molecular mechanism of these two related phenomena, however, is not yet clear.

The pulse-induced disturbance of the membrane structure is a microsecond process. Only those regions of the membrane that oppose the external electrodes are expected to be perturbed (see Theoretical Background). Analysis of the process therefore requires high resolution both temporally and spatially. Thus we have constructed a pulsed-laser fluorescence microscope with a submicrosecond imaging capability, with which the instant of pore formation has successfully been imaged. Here we report the major results and their interpretation.

Dr. Ashikawa's present address is ESR Center, Medical College of Wisconsin, 8701 Watertown, Plank Road, Milwaukee, WI 53226.

Correspondence should be sent to Dr. Ikegami.

METHODS

Theoretical Background

One point that has been established about the pore formation and fusion is that the direct cause is the field-induced transmembrane potential (1, 2). Under an external electric field the potential drop across a cell is sustained by the cell membrane, which is a poor conductor, while the field in the ion-rich cell interior becomes zero. Thus, when a field E is turned on at time $t = 0$, the induced membrane potential Ψ (outside vs. inside) at polar coordinate θ (with respect to the axis pointing to the anode) is given by

$$\Psi(\theta, t) = 1.5\, aE \cos\theta[1 - \exp(-t/\tau)] \quad (1)$$

$$\tau = aC_m(r_i + r_e/2), \quad (2)$$

where a is the cell radius, C_m the membrane capacitance per unit area, r_i and r_e the specific resistances of the intracellular and extracellular media (3). The rise time τ is of the order of 1 μs or less (3). An electric pulse for which $|\Psi|$ exceeds a critical value, ~1 V in most cells (1, 2), produces pores in the cell membrane (1, 4). Pore formation is fast; duration of the supracritical Ψ can be as short as 1 μs (5, 6).

In Eq. 1 the membrane conductance G_m is assumed to be negligible, an assumption valid with normal cells (3). If G_m is finite (and uniform over the entire membrane), the membrane potential Ψ in Eq. 1 (and also τ) is reduced in proportion to the following factor (3).

$$f = 1/[1 + aG_m(r_i + r_e/2)]. \quad (3)$$

Thus, if the pores introduce appreciable membrane conductance, a reduction in Ψ is expected. The θ dependence in Eq. 1, however, suggests that $|\Psi|$ will exceed the critical value only for θ around 0 and 180°. Only those membrane regions that oppose the external electrodes will be perforated and give rise to a finite G_m. If this G_m is large enough, then the perforation will be detected as a drop in $|\Psi|$ mainly around the two poles at

θ = 0 and 180°. Flattening at the peaks of the cos θ dependence is expected.

For a nonuniform (θ-dependent) G_m, the potential Ψ cannot be given in an analytical form. To compare with experiment, therefore, we calculated the steady-state solution $\Psi(\theta, t = \infty)$ as a numerical solution of an appropriate Laplace's equation with a boundary condition including the $G_m(\theta)$ (details will be described elsewhere). We assumed that $G_m(\theta)$ is given by

$$G_m(\theta) = \begin{cases} G_o(|\cos\theta| - \cos\theta_c)/(1 - \cos\theta_c) \\ 0 \end{cases}$$

$$(\theta \le \theta_c,\ 180° - \theta_c \le \theta)$$

$$(\theta_c < \theta < 180° - \theta_c), \qquad (4)$$

where G_o is a constant (maximal conductance) and θ_c is the angle at which the potential in the absence of pores, 1.5 aE cos θ, would become 1 V. Eq. 4 implies that G_m in the perforated region is proportional to the excess potential, $|1.5\ aE \cos\theta| - 1$ V. This rather arbitrary choice reproduced the experimental results fairly well (see Results).

Pulsed-Laser Fluorescence Microscope

Experimentally, spatial resolution of Ψ, though at steady state, has been achieved by the use of voltage-sensitive fluorescent dyes combined with video microscopy (7). Time resolution of video by itself, however, is poor. Ψ has been time resolved with a photomultiplier tube (8), but the imaging capability was sacrificed. To observe $\Psi(\theta, t)$ as images at microsecond resolution, therefore, we used a pulsed dye laser (model DL-1400, Phase-R, New Durham, NH) with a pulse duration of 0.3 μs as the excitation source for the dye fluorescence. We stained the cell membrane of a sea urchin egg with the dye RH292, of which the fluorescence intensity changes linearly with membrane potential (9). The egg illuminated with a single pulse from the laser produced a fluorescence image of sufficient intensity on a video camera (SIT type C1000-12, Hamamatsu K. K., Hamamatsu, Japan). The laser was triggered during a vertical blanking period of the camera. The instantaneous image stored as charge distribution on the target plate of the camera was output at ordinary video rate into a digital image processing system (C2000, Hamamatsu K. K.). By synchronizing the laser with the electric pulse applied to the egg we were able to take a snap shot of the voltage response of the cell membrane at a desired time in the pulse.

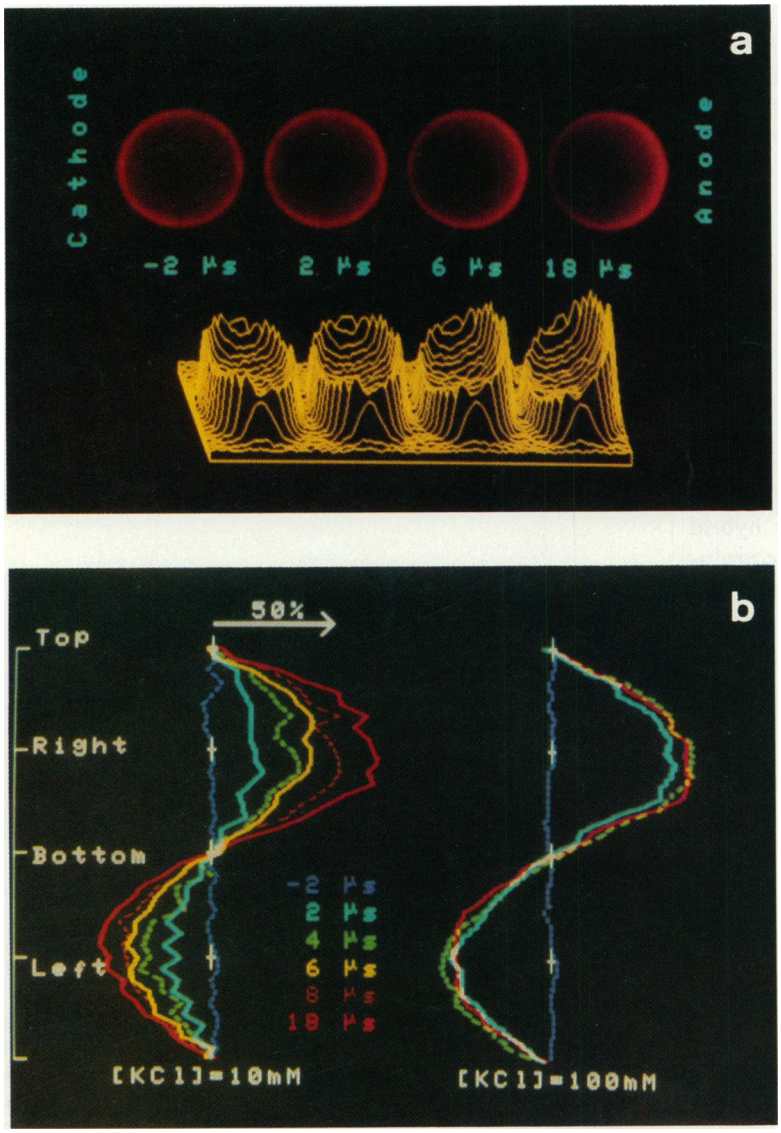

FIGURE 1 Rise of transmembrane potential in a pulsed electric field. (*a*) Images of red fluorescence (intensity profiles in yellow), from a sea urchin egg stained with the voltage-sensitive dye RH292, obtained at indicated times after the onset of a square-wave electric pulse (100 V/cm, duration 25 μs). (*b*) Profiles of the fluorescence response, relative to the intensities at zero field, along the circumference of the cell at indicated times, clockwise starting from the top of the cell. Bathing medium, 10 mM KCl, 1 mM $MgSO_4$, 0.1 mM Tris (pH 7.8), 1.2 M glucose, and 3 μM RH292; the medium in *b*, right, the same except [KCl] = 100 mM, [glucose] = 0.8 M. Temperature, 20°C. In a separate experiment the fluorescence change was shown to be approximately proportional to the field intensity E for E up to 133 V/cm.

Experimental Procedures

Unfertilized eggs of sea urchins *Hemicentrotus pulcherrimus, Temnopleurus toreumaticus, Anthocidaris crassispina,* or *Clypeaster japonicus* (results indistinguishable) were washed in a desired medium (see figure legends) and resuspended in the same medium containing 3 μM RH292 (Molecular Probes, Inc., Eugene, OR). The suspension was introduced in a 1-mm gap between a pair of platinized platinum electrodes on a cover glass. A selected egg was illuminated on an inverted epifluorescence microscope (ICM-405, Carl Zeiss Inc., Tokyo), with a light pulse (540 nm) from the dye laser. Several successive images, each under a differently conditioned electric pulse, were taken at intervals of 2 s from the same egg.

RESULTS AND DISCUSSION

Rise of Membrane Potential

Fig. 1 *a* shows the response of an egg to a subcritical electric pulse. The dye RH292 fluoresced strongly when bound to the cell membrane, giving a circular image in the absence of external electric field. When the external field in the direction from right to left in Fig. 1 *a* was turned on, the fluorescence in the region facing the anode increased with time whereas an opposite response was observed in the region facing the cathode. Plotted in Fig. 1 *b*, left, are the intensity profiles along the cell circumference at selected instants. Although the profiles are rather noisy, each profile is approximately a cos θ curve as predicted in Eq. 1.

For sea urchin eggs the parameters in Eqs. 1 and 2 are $a = 50\ \mu$m, $C_m \sim 1\ \mu$F/cm^2, and $r_i \sim 200\ \Omega \cdot$ cm (3, 10). At $E = 100$ V/cm (Fig. 1 *a*) the maximal potential $\Psi_{max} \equiv \Psi(\theta = 0°, t = \infty) = 1.5\ aE$ is 0.75 V, lower than the critical potential of ~1 V for the pore formation in the cell membrane of sea urchin eggs (11). With $r_e = 1.2\ k\Omega \cdot$ cm for the bathing medium the rise time τ is calculated to be ~4 μs. The circumferential profiles in Fig. 1 *b*, left, show that the potential Ψ rose with the predicted time constant.

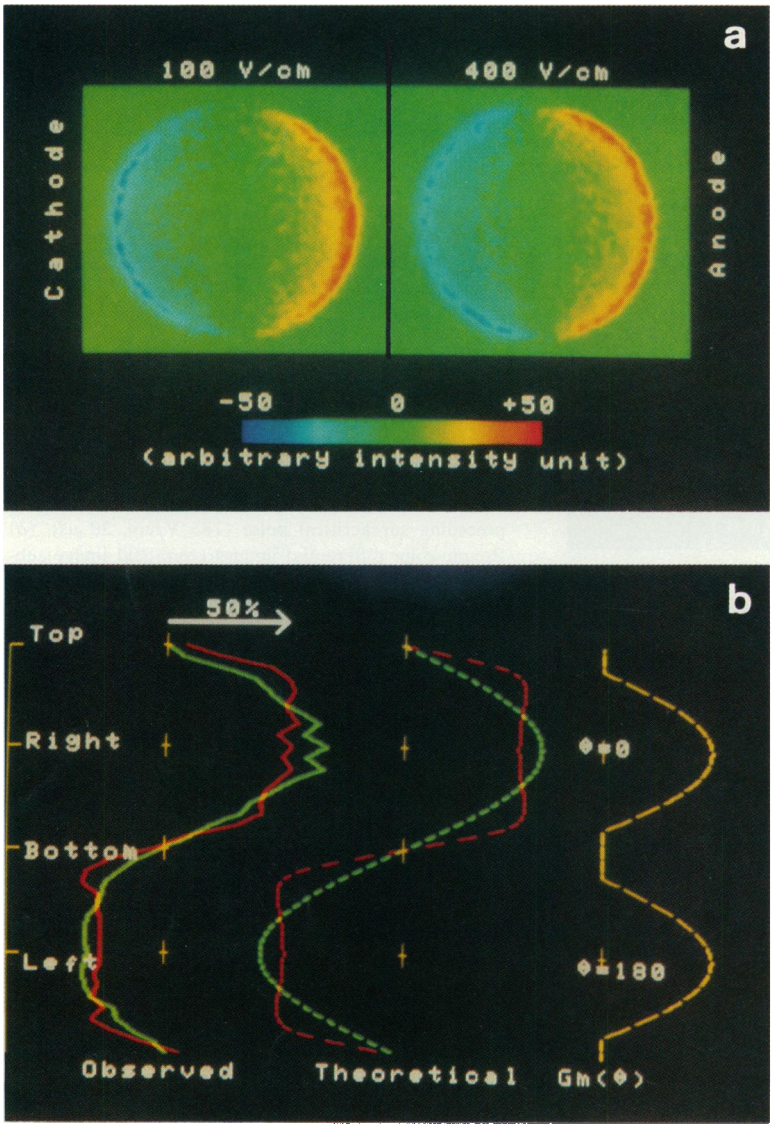

FIGURE 2 Responses, at 20 μs, to a subcritical (100 V/cm) and supracritical (400 V/cm) electric pulse of duration 25 μs. (*a*) Pseudo-color representation of the differential images (zero-field image subtracted). (*b*) Circumferential intensity profiles. Green, at 100 V/cm; red, at 400 V/cm. The dashed profiles are theoretical: green, Eq. 1 with $E = 100$ V/cm and $t = \infty$; red, at $E = 400$ V/cm with $G_m(\theta)$ given by Eq. 4 where $\theta_c = 70°$ and $G_o = 1.2$ S/cm^2; yellow, the shape of $G_m(\theta)$. Bathing medium as in Fig. 1 *a* ([KCl] = 10 mM).

An immediate rise, in contrast, was observed in high-salt medium (Fig. 1 *b*, right) where $r_e = 120\ \Omega \cdot$ cm and where the predicted $\tau \sim 1\ \mu$s. The data also show that the response time of the dye RH292 was within 2 μs. When the external field was turned off the induced potential decayed with the same τ as in the rising phase. Thus, for moderate field intensities we have been able to demonstrate the validity of Eqs. 1 and 2, which early in this century played a key role in elucidating electrical properties of cells and particularly of cell membranes (3).

Pore Formation

The $\cos\theta$ dependence was no longer observed at field intensities above the critical value of 133 V/cm for which $\Psi_{max} = 1$ V. The top of the circumferential profile became flat or even slightly concave as is seen in Fig. 2, where the responses to subcritical ($E = 100$ V/cm, $\Psi_{max} = 0.75$ V) and supracritical ($E = 400$ V/cm, Ψ_{max} would have been 3 V) pulses are compared. Apparently rise of the transmembrane potential beyond the critical value was counteracted by the increase in the membrane conductance resulting from the pore formation. In fact the experimental profile at 400 V/cm was well simulated by a theoretical one (Fig. 2 *b*) in which the membrane conductance G_m was assumed to be given by Eq. 4 with $\theta_c = 70°$ and $G_o = 1.2$ S/cm^2. The fit supports the idea that only those regions where $|\Psi|$ had exceeded 1 V, i.e., the regions within θ_c from the two poles opposing the electrodes, were perforated. The value of G_o, the membrane conductance at the two poles, is orders of magnitude higher than the conductance of normal egg membrane which is well below 10 mS/cm^2 (3, 10). (That G_o should be $\gtrsim 1$ S/cm^2 may also be seen from Eq. 3. For large θ_c, the reduction in Ψ at the poles is described, very approximately, by the factor f.) The above G_o corresponds to the replacement of as much as 0.01–0.1% of the membrane area by aqueous openings. The enormous leakiness, if it persists, would cause immediate rupture of the cell. The membrane must be highly disorganized, which

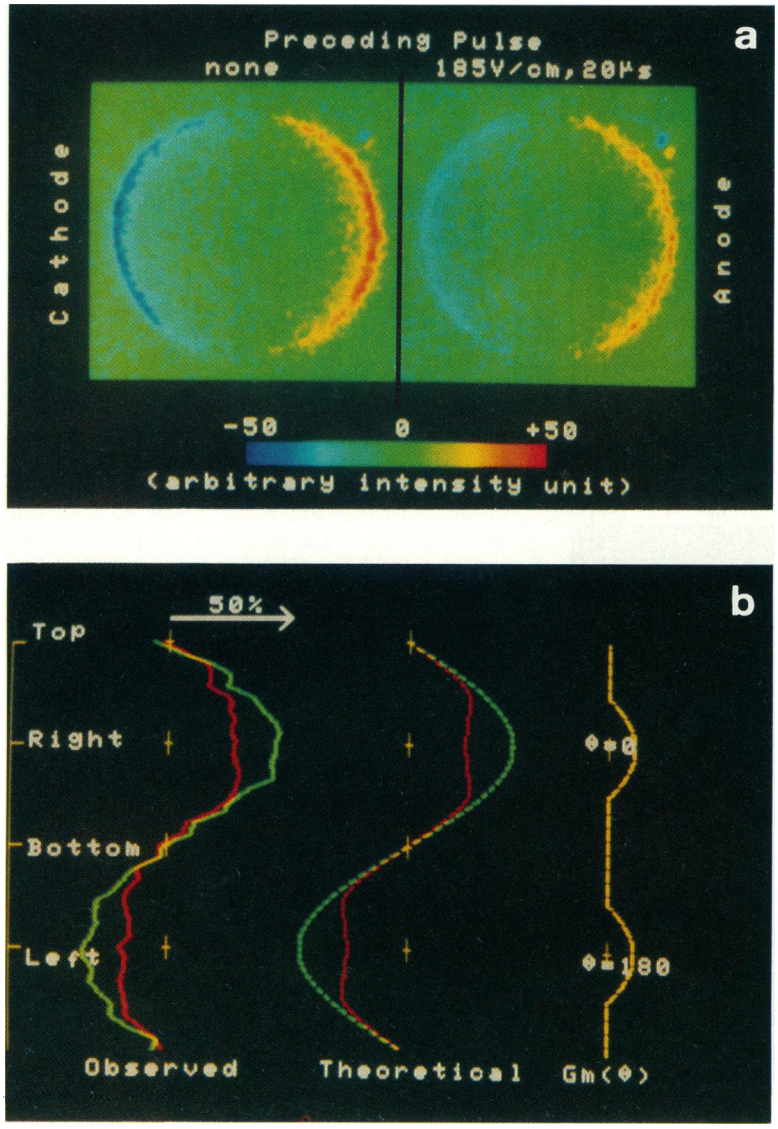

FIGURE 3 Responses, at 12 μs, to a monitor pulse (67 V/cm, 15 μs) in the absence of, and 20 μs after, a preceding supracritical pulse (185 V/cm, 20 μs). (*a*) Pseudo-color differential images (zero-field image subtracted). (*b*) Circumferential intensity profiles. Green, without; red, with the preceding pulse. The dashed profiles are theoretical: green, Eq. 1 with $E = 67$ V/cm and $t = \infty$; red, at $E = 67$ V/cm with $G_m(\theta)$ given by Eq. 4, where $\theta_c = 44°$ and $G_o = 0.3$ S/cm^2; yellow, the shape of $G_m(\theta)$. Bathing medium as in Fig. 1 *a* ([KCl] = 10 mM).

may well initiate the electrofusion process. A similar conductance value has been suggested, indirectly, for erythrocyte under a supracritical field (6).

The possibility that the flattening at the top of the profile might have been due to saturation of the dye response per se was ruled out by a double-pulse experiment, in which response to a subcritical electric pulse of constant intensity (monitor pulse) was examined with and without a preceding pulse. The response was unaffected by the preceding pulse as long as the intensity of the preceding pulse remained below the critical value. After a supracritical pulse, however, the response to the monitor pulse became lower and flattened (Fig. 3). This clearly demonstrates that the degraded response at high fields reflected a structural change (pore formation) in the cell membrane, and that the change persisted after the field was turned off. (Note, however, the possibility that this persisting effect may well have been amplified by the monitor pulse. The value of G_m estimated from Fig. 3 [see legend] may be much larger than the G_m at zero field.)

The effect on the monitor pulse decayed rapidly after the termination of the preceding pulse, becoming barely observable at 500 μs. At 2 s the effect apparently disappeared. The pores shrank rapidly as has been suggested (6). The recovery, however, was not complete. Often, cells treated with an intense and long pulse (e.g., 400 V/cm, 100 μs) eventually swelled and burst, due presumably to the osmotic imbalance caused by the leakage of ions and small molecules through the shrunken but still open pores (1, 5). The final pore size has been shown to be controllable (4).

Time course of the pore formation was examined in the high-salt medium where the rise of the potential was fast. The circumferential profiles 1 or 2 μs after the onset of a supracritical pulse were already low and flattened, indicating that the pores were formed within 1 μs. The cell membrane cannot sustain a potential greater than the critical value even for a short period of time. Profiles later in the pulse were lower than the early profiles, but the difference was rather small ($\lesssim$20% drop over 20 μs). Once the induced potential drops below the critical value the increase in G_m slows down. The transmembrane current ($=\Psi/G_m$) sustained at the high level, however, probably continues to accumulate in the membrane some strain which interferes with the later shrinkage of the pores. The pore radius long after pulsation has been shown to be highly sensitive to the pulse duration (4, 5).

CONCLUDING REMARKS

We have shown that an enormously leaky state is realized in those regions of cell membrane that are under a supracritical potential and that the membrane recovers quickly after the external field is removed. The kinetics can be controlled by the size of the applied pulse and optionally by subsequent pulses. These results should be useful in designing successful cell manipulation techniques, such as the introduction of high-molecular weight materials in cells by an electric pulse.

The work presented is the first application of the pulsed-laser fluorescence microscope. The pulsed illumination system should be useful in many other applications where imaging at a (sub-)microsecond time resolution is required. Here we have examined fast events induced by an electric pulse. Another important field will be the imaging of processes induced by a light pulse. Responses to the light itself as well as those to photochemical products can be studied. Progress is being made toward this goal.

We thank Drs. K. Hirano, Y. Toyoshima, T. M. Noumura, I. Mabuchi, S. Yonemura, I. Yasumasu, Y. Tanaka, Y. Hiramoto, Y. Yoshimoto, H. Hosoya, K. Ohta, A. Ikai, Y. Amari, and M. Hosoda for useful suggestions and the gift of sea urchins.

Supported by special coordination funds for promoting science and technology from the Agency of Science and Technology and by grants-in-aid from the Ministry of Education, Science, and Culture.

Received for publication 27 November 1987.

REFERENCES

1. Tsong, T. Y. 1983. Voltage modulation of membrane permeability and energy utilization in cells. *Biosci. Rep.* 3:487–505.
2. Zimmermann, U. 1982. Electric field-mediated fusion and related electrical phenomena. *Biochim. Biophys. Acta.* 694:227–277.
3. Cole, K. S. 1972. Membranes, Ions and Impulses. University of California Press, Berkeley.
4. Kinosita, K., Jr., and T. Y. Tsong. 1977. Formation and resealing of pores of controlled sizes in human erythrocyte membrane. *Nature (Lond.).* 268:438–441.
5. Kinosita, K., Jr., and T. Y. Tsong. 1977. Voltage-induced pore formation and hemolysis of human erythrocytes. *Biochim. Biophys. Acta.* 471:227–242.
6. Kinosita, K., Jr., and T. Y. Tsong. 1979. Voltage-induced conductance in human erythrocyte membranes. *Biochim. Biophys. Acta.* 554:479–497.
7. Gross, D., L. M. Loew, and W. W. Webb. 1986. Optical imaging of cell membrane potential changes induced by applied electric field. *Biophys. J.* 50:339–348.
8. Ehrenberg, B., D. L. Farkas, E. N. Fluhler, Z. Lojewska, and L. M. Loew. 1987. Membrane potential induced by external electric field pulses can be followed with a potentiometric dye. *Biophys. J.* 51:833–837.
9. Grinvald, A., R. Hildesheim, I. C. Farber, and L. Anglister. 1982. Improved fluorescent probes for the measurement of rapid changes in membrane potential. *Biophys. J.* 39:301–308.
10. Hiramoto, Y. 1959. Electric properties of Echinoderm eggs. *Embryologia.* 4:219–235.
11. Baker, P. F., D. E. Knight, and M. J. Whitaker. 1980. The relation between ionized calcium and cortical granule exocytosis in eggs of the sea urchin *Echinus esculentus. Proc. R. Soc. Lond. Biol. Sci.* 207:149–161.